Tarrah et al. / Iranian Journal of Earth Sciences 7 (2015) /114-123

Islamic Azad University
Mashhad Branch

Mineralogical and geochemical investigations of chromite ores from ophiolite complexes of SE Iran in terms of chrome spinel composition

Jamal Tarrah[1*], Zahra Abedpour[1], Karl Strauss[2], Thomas Schirmer[2], Kurt Mengel[2]

1. Islamic Azad University, Bandar Abbas Branch, Geology Department, Bandar Abbas, Iran
2. Institute of Mineralogy-Geochemistry and Salt Deposits, University of Clausthal, Germany

Received 16 December 2014; accepted 20 February 2015

Abstract

Ten chromite ores from ophiolite complexes in SE Iran were analyzed mineralogically by XRD, chemically by XRF, and mineral chemistry by EPMA. The identified paragenesis of silicate minerals of chromite ores with the X-ray diffraction is pronounced differently. It consists of secondary phases formed as serpentine, Cr-containing chlorite (kaemmererite), chromic garnet (uarovite) with preserved partly primary minerals of peridotite parent rocks such as olivine and diopside. From the total chemical analysis by XRF results, a good correlation exists between the Cr_2O_3 and SiO_2 content (as an index of the sum of the silicate minerals). This allows an easy decision for mine ability of chrome ores. In a relatively good correlation are also the Mg and Fe oxide contents. The mineral chemisty (EPMA analysis) of spimel mineral provides valuable information about the the octahedral layer of the spinel,. The results of the microprobe analysis show a variation in the chemical composition of the spinel phase of a mixed crystal formation consisting of: chromite ($Fe^{2+}Cr_2O_4$), magnesiochromite ($MgCr_2O_4$), spinel ($MgAl_2O_4$), and hercynite ($Fe^{2+}Al_2O_4$). This becomes even more complex by the mixed crystal relationship with picotite [$(Mg, Fe^{2+})(Cr,Al,Fe^{3+})_2O_4$], which contains Fe^{3+} in the tetrahedral position. The chrome spinel vary inCr-numbers [100 ×(Cr / Cr + Al) = 75-92] and Mg-numbers [100 * (Mg / Mg + Fe^{2+}) = 38-57]. The partition of iron between Fe^{3+} und Fe^{2+} was made by assuming normal spinel structure, using the formula AB_2O_4. Correlations of microprobe analysis indicate that the mineral chemistry of the studied spinel is characterized mainly by the divalent elements of Mg and Fe^{2+} in the A position and trivalent elements Cr and Al in the B position.

Keywords: *Ophiolite, Mineralogy, Chemical Composition, Microprobe, Spinel, SE Iran*

1. Introduction

Metal-bearing deposits with economic value play an important role in modern industry. In this connection, the chromium- deposits are economically important. For example, Bushveld Cr deposits (stratiform chromite deposits) are one of the most important sources of ore deposits on Earth and have long been known with little deposits of Precambrian formations. In contrast are the much small podiform chromite deposits that are spatially more widespread. These Cr-rich lenses are irregularly shaped and form about 4% of world reserves (Okrusch and Matthes 2013). They are located in deformed ultramafic rock units of the ophiolite complexes and derived from the geologically younger Phanerozoic. Since these Cr-rich glasses lie in ophiolite formations, their origin genetically by many authors (Glennie et al. 1990; Glennie 2000; Ghazi et al. 2004) have been traced back to former intrusion in marginal basins of oceanic crust (back-arc basin).

From an economic point, this podiform chromite from Iran, after its iron and copper ore deposits, are the third most important source of raw material under the metal deposits. Therefore, these ophiolite complexes were recently the subject of several recent studies (Moghtaderi et al. 2003; Bagherian and Tourchi 2004; Emamalipour 2008; Rajabzadeh and Moosavinasab 2012; Rajabzadeh and Moosavinasab 2013). The focus of these studies was mostly the study of the PGM and PGE-compounds and the detection of other rare elements.

In the present study, the mineralogical characteristics and chemical features of 10 chrome ore samples from ophiolite complexes in southeast Iran have been discussed. The detection of the mineralogical composition by XRD was followed by the overall chemical analysis by XRF. This paper demonstrates microprobe analysis for both spinel and the coexisting silicates. The interrelationship between the chromite and its chemical dates as well as the associated silicates, have been described. The chemical composition of associated silicates has been studied in detail (Tarrah and Abedpour 2014), so they are briefly discussed here.

---

*Corresponding author.
E-mail address (es): jamaltarrah@iauba.ac.ir

2. Sample material and methods of investigation

2.1. Ore samples

The selected samples were taken from three ophiolite complexes (Esfandagheh-Dolatabad (ES), Chehelkureh (TK), and Bazman (BZ)) in southeastern Iran. Their location and the macroscopic description of the extracted ore samples are shown in Table 1 and Fig 1. All studies were performed in the Institute of Mineralogy-Geochemistry and Salt Deposits (Department of Repository Research of the Technical University of Clausthal, Germany). The samples were separated from the ophiolite complexes by a hand piece and the following preparations were done: preparations for powder XRD, melting tablets for XRF, and polished sections for microprobe analysis.

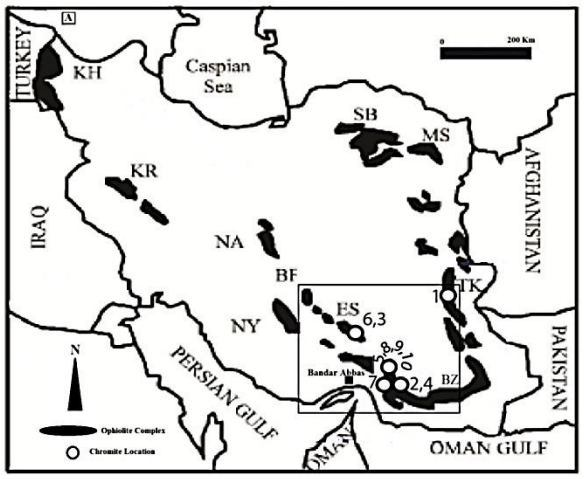

Fig 1. Distribution map of ophiolithe complexes in Iran (KH: Khoye, KR: Kermanshah, NA: Naein, BF: Baft, NY: Neyriz, ES: Esfandagheh, BZ: Bazman, TK: Chehelkureh, MS: Mashhad, SB: Sabzewar) with sampling points for the core samples (number 1-10);

2.2. Analytical methods

2.2.1. XRD

Diffractograms were recorded by XRD to identify the mineral phases that occurred in the samples. The samples were previously crushed mechanically. The pulverization was carried out manually with an agate mortar. The sample powder was mixed with pure CaF_2 (20 wt. %) in order to correct the results from the measurement height errors. For the recording of the diffraction patterns, back loading preparations were made. An X-ray diffractometer PANalytical X pert pro type with copper tube was used as a device. The device settings were 40 kV and 40 mA. In Table 2 (section 4.1), the X-ray was used to qualitatively determined, and identified the data compared with the microprobe analysis of mineral phases, and the d values of the (113) reflections of the corresponding spinel phases are listed.

2.2.2. XRF

To determine the bulk-rock composition an Axion PANalytical XRF spectrometer with super Q5 was used. The samples were mixed because of the high Cr content first with a rock crystal powder SiO_2 (from the collection of the Institute) in a ratio of 1:4 and fused with $Li_2B_4O_7$ in a ratio of 1:6 at 1100 °C. The melting tablets were used to determine the main as well as the trace elements and 30 elements were co-analyzed. Fifteen trace elements at levels of 0 to 0.05 wt. % and Na_2O/K_2O with zero percent were taken out here. In Table 3 (section 4.2), the measurement results are shown.

2.2.3. Microprobe analysis

The chemical composition of chromite and its variation width was obtained from a four-channel CAMECA SX 100 electron microprobe. Beside chromite, coexisting silicates were also analyzed. Polished sections were made with very high quality. The vapor deposition, to maintain the conductivity was carried out with carbon. The following instrument settings were used for the measurements:

Acceleration voltage: 15 kV

beam current: 40 nA

Electron beam diameter: 5 µm

The chemical homogeneity of the chromite and silicate grains was confirmed by several microprobe traverses. For the measurement of all elements Kα line was taken as a basis. For the measurement of the elements following standard minerals were used: hematite (Minas Gerais, Brazil) for Ti / Fe, Kaersutite - Kakanui (Jarosewich) for Ca and Si and chromium dioxide (syn.) for Cr. Table 4 lists the structural formulas of spinel phases from the microprobe data based on the formula $A^{+2}B_2^{3+}O_4$.

2.2.4. Determination of the structural formulas for spinel phases

Table 4 lists the structural formulas of spinel phases determined from the microprobe data based on the formula $A^{+2}B_2^{3+}O_4$. Because shares of divalent and trivalent iron were analytically indistinguishable, a purely mathematical division was carried out: In the B-position (tetrahedral layer), the Al and Cr shares were added and made up its sum with iron up to 2.00. The balance of Fe accounted for as Fe^{2+} on the A-site (octahedral) and should theoretically result in a value of 1.00 for the sum of Fe, Mg, Mn and Ni content. Deviation from the modal formula ($A^{+2}B_2^{3+}O_4$) is negligible and is mainly due to an excess of A^{2+}. It is also probably due to the microprobe analysis or a rounding error.

Table 1. Sample description and sample numbers with location and a macroscopic description

Sample Name	SampleNno.	Location	Macroscopic Description
ZNG	1	Nosratabad	massive Cr-ore with olivine
NJ	2	Manujan	massive Cr-ore
RX	3	Esfandagheh-Dolatabad	Cr-ore with banded olivine
MJ	4	Manujan	massive Cr-ore with serpentine
FB	5	Faryabmine	nodular Cr-ore
SF	6	Esfandagheh-Dolatabad	massive Cr-ore
RB	7	Barantin-Rudan	massive Cr-ore with chlorite
FAR 3	8	Faryabmine	Pretreated Crore
FAR 1	9	Faryabmine	Cr-ore with green coating
FAR 2	10	Faryabmine	Powder of Cr-ore

Table 2. The mineral composition of the Cr ores and identifying different spinel phases on the basis of the d-values of the diagnostic (113) reflection

Sample Name	Sample No.	Mineralogical composition	$d_{(113)}$-Value (Å)
ZNG	1	Cr-Phase, Serpentine, Olivine	2.50390
NJ	2	Cr-Phase, Chlorite, Uvarovite	2.48848
RX	3	Cr-Phase, Serpentine, Olivine	2.50431
MJ	4	Cr-Phase, Serpentine, Pyroxene	2.49806
FB	5	Cr-Phase, Olivine, Pyroxene	2.50441
SF	6	Cr-Phase, Serpentine, Chlorite,	2.50477
RB	7	Cr-Phase, Chlorite	2.50498
FAR 3	8	Cr-Phase, Serpentine, Chlorite,	2.50556
FAR 1	9	Cr-Phase, Chlorite, Uvarovite	2.50186
FAR 2	10	Cr-Phase, Serpentine, Olivine	2.50592

3. Geological Setting

Iran is a mosaic of continental terranes from the Cadomian (520-600 Ma) age, stitched together along sutures decorated by Paleozoic and Mesozoic ophiolites. Mesozoic ophiolites of Iran are mostly Cretaceous in age and are related to the Neotethys and associated back arc basins on the S flank of Eurasia. Most Mesozoic ophiolites of Iran show supra-subduction zone (SSZ) geochemical signatures, indicating that SW Asia was a site of plate convergence during the Late Mesozoic time (Shafaii Moghadam and Stern 2015). The Iranian Makran is an accretionary prism developed above a North-dipping subduction zone subducting the Indian Ocean crust (Siddiqui et al. 2012).

Eight studied samples (except samples 6 and 3) are located in the Makran zone. The Makran accretionary prism extends for 450 km, from SE Iran to SW Pakistan. Makran comprises a region about 200 km wide in SE Iran between the Jaz Murian depression and the Gulf of Oman. In the north, in the Chagai and RasKoh mountain ranges, there are rock sequences that represent the associated magmatic arc (Siddiqui et al. 2012). There are three important zones in Iranian Makran, from S to N: (1) the Makran accretionary prism, which continues to form as a result of subducting the Indian plate and the sediments on it beneath the central Iranian block, (2) the Jaz Murian depression, which may be a sediment-filled Mesozoic back-arc basin (McCall and Kidd 1982; Glennie et al. 1990; McCall 1997) or an intra-arc basin (Shahabpour 2010), and (3) Cenozoic volcanic and plutonic rocks of andesitic to rhyolitic composition, which reflect arc magmatism related to the Makran subduction system. The region below the ophiolites were divided into two parts:(1) Makran ophiolites including Jurassic-Early Paleocene Rameshk- Mokhtarabad and colored mélange complexes, and (2) Kahnuj ophiolite, which is the NW continuation of the Inner Makran ophiolite belt (Shafaii Moghadam and Stern 2015). Most of studied samples are located in the outer Makran ophiolite belt. The outer Makran ophiolites include two relatively

intact ophiolites: the Sorkhband and Rudan complexes (McCall 1985), which are 17 km long and 9 km wide, and composed mainly of dunite, harzburgite and stratiform-type chromitite with pyroxenite/ wehrlite sill-like intrusions and minor isotropic to coarse-grained gabbros at the top of the sequence. This complex shows faulted contact with Bajgan-Durkan metamorphic rocks (Shafaii Moghadam and Stern 2015). Biomicrites intercalated with outer Makran pillow lavas are dominated by Campanian-Maastrichtian micro faunas, although there are also Cenomanian, Turonian, Coniacian, and Santonian microfossils (McCall 2002). Radiolarites associated with pillow lavas and pelagic limestones range from Pliensbachian (Jurassic) to Coniacian.

4. Results

4.1. The mineral composition of ore samples

The mineralogical characteristic of a podiform chromite deposit is governed by the rock mantle composition, the degree of partial melting of these rocks and selective removal of minerals under different thermodynamic conditions. Particularly the formation of chromitites is dictated by a combined process of partial melting and melt/rock interaction in the mantle (Zhou et al. 1996) as well as by the process of the fractionation (fractional crystallization). It is generally accepted that the progressive differentiation of oxide-rich melt from mafic magma leads the concentration of Cr in chromitites (Rajabzadeh and Moosavinasab 2012). The variation in mineralogy of podiform chromite deposits is also an indicator to understand not only processes in the upper mantle and magmatic evolution through past time, but also provides a mirror for the post-magmatic events such as chemical weathering. The secondary silicate minerals reflect, for example, depending on their origin, the intensity and the properties of the chemical weathering process.

Based on the examination with the XRD and microprobe, the bulk mineralogy of chrome ores consist of, in addition to spinel of two major groups: (a) the association of partly preserved primary minerals of the peridotite parent rocks such as olivine and diopside and (b) the secondary phases such serpentine, Cr-containing chlorite (kaemmererite) and chromiferous garnet (uvarovite) as shown in Table 2. By far the most common silicates in chromium ores, are serpentine and chlorite. The ores included with the exception of samples 5 and 7, usually two silicate minerals. Sample 5 contains three silicate minerals and sample 7 only one. As Table 2 shows, the investigated ores are mineralogically divided into six groups as follows:

Cr-rich spinel, olivine and serpentine group (samples 1, 3, 10)

Cr-rich spinel, diopside and serpentine group (sample 4)

Cr-rich spinel, diopside and olivine and chlorite group (sample 5)

Cr-rich spinel, chlorite and serpentine group (samples 6 and 8)

Cr-rich spinel, chlorite and uvarovite (samples 2 and 9)

Cr-rich spinel and chlorite (sample 7)

As can be seen from Table 2, the spinel marked differences in the position of the (113) reflections. The values are in the range of d = 2.48848 - 2.50592 Å. The reflex shift is a first indication of the different mineral chemistry of spinel phases (the importance of these phenomena will be discussed by a forthcoming paper). As previously mentioned in the introduction, the chemical composition of the silicate phases as part of a work (Tarrah and Abedpour 2014) has been recently reported. The average values of the chemical data are taken over in this work (Table 5) and discussed in relation to the mineralogical composition of item a): existing primary minerals and b) the secondary phases.

a) Primary minerals

As an example, a BSE image of olivine in Fig 2 is shown. Olivine provides a lighter color than serpentine. Forsterite content (Fo) of olivine is calculated by the formula: Fo = [(Mg X 100) / (Mg + Fe_{total})]. Fo of olivine varies between 84.8-93.0, averaging 89.9 (Tab. 3). The maximum content is more or less the same with the highest value for MgO content, that for mantle rocks in the dunite (94.7 wt. %), harzburgite (91.6 wt. %) and lherzolite (91.5 wt. %) was reported from southern Iran in Neyriz ophiolite (Rajabzadeh and Moosavinasab 2012). The minimum value of 84.8 is due to the low MgO content in sample 10 (Tarrah and Abedpour 2014). NiO in olivine ranges between 0.3 and 0.7 wt. %, averaging 0.5. The concentration of Al, Cr, Ca and Mn is negligible.

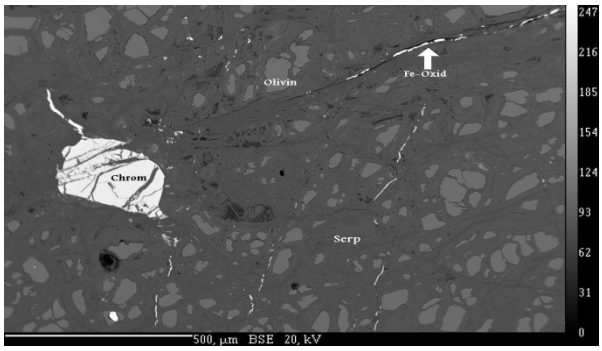

Fig 2. BSE image of sample no. 10 of the mine Faryab, combined with the mineral chromite

According to the theoretical formula of diopside ($Ca_{0.5}Mg_{0.5}$ SiO_3) the amount of calcium, magnesium and silica oxide, respectively, are 25.9, 18.5 and 55.6 percent, and when these were compared with the average of the amount,which are specified in Table 5,

pyroxene composition in sample 4 and 5 is diopsidic. Wollastonite content (Wo) of diopsid, was calculated by the formula: Wo = [(Ca X 100) / (Wo + En)], is 57.1 (Tab.3). This value is similar to the theoretical value of wollastonite (58.5) in diopside with the formula ($Ca_{0.5}$ $Mg_{0.5}$) SiO_3. The amount of iron oxide as a component of orthopyroxene is just 1.0 percent (Table 5). Other oxides values are below one percent.
Since orthopyroxenes usually undergo lower serpentinization as olivine, orthopyroxene in the presence of harzburgite as a frame stone should still be present. This is not the case, according to the results of the phase analysis. From the above it can be concluded that the harzburgite should not be the only frame stone. The occurrence of clinopyroxene was to be regarded either as a component of dunite or as exsolution of orthopyroxene in harzburgite, if it existed.

b) Secondary minerals

Serpentine is one of the main secondary minerals in most ultrabasic rocks. Serpentine can be identified by its dark gray color from the mineral olivine with gray toning (Fig 2). Assuming the presence of olivine (forsterite) and enstatite as an origin, the reaction is as follows (Lameyre 1986):

(1) $2Mg_2\,SiO_4 + Mg_2\,Si_2O_6 + 4H_2O \longleftrightarrow Mg_6Si_4O_{10}\,(OH)_8$

Is a silicate mixture with less Si present, for example, only forsterite the serpentine weathering product may be accompanied by brucite:

(2) $4Mg_2\,SiO_4 + 6H_2O \longleftrightarrow Mg_6\,Si_4O_{10}\,(OH)_8 + 2Mg\,(OH)_2$

For the formation of serpentine, the reaction 2 is without the phase enstatite, which we do not consider as a primary mineral, more likely. The data in Table 5 shows the mechanism of the alteration. The average content of olivine and serpentine oxides of Table 5 are expressed as follows:

(3) Olivine: 41.1 % (SiO_2) +52.5% (MgO) +5.9% (FeO) +0.5% (NiO) = 100.0 %

(4) Serpentine: 40.1% (SiO_2) +41.9 %(MgO)+2.5% (FeO)+0.3% (NiO) = 84.8 %

The difference between the oxide contents in olivine oxide (100.0 wt. %) and serpentine (84.8 wt. %) is 15.2 wt. %. This value is approximately equal to the amount of the difference between 100 and the value for the total sum of all oxides in serpentine (100-85.8=14.2). Interestingly, the amount of H_2O for the serpentine is theoretical 13 wt. %.

In addition to the serpentine, chlorites are also altered products. Figure 3 shows the BSE image of chromitite with chlorite from Barantin-Rudan. These Cr-bearing chlorites are known as kaemmererite(Mussallam et al. 1981) explained the formation of chromium-containing chlorite (up to 2.5 wt. % Cr_2O_3) with a remobilization of Cr and subsequent accumulation of iron. In this study, the chlorites have Cr_2O_3 content up to 5.1 wt. %, averaging 3.1 (Table 5). Due to the high content of magnesium (31.8-36.6 wt. %, averaging 35.1), the chlorite is definitely trioctahedral with a very low content of Fe (0.4 –3.4 wt. %, averaging 1.3) and the amount of aluminum oxide ranges from about 14 to 18%, averaging 15.1 (Table 5).

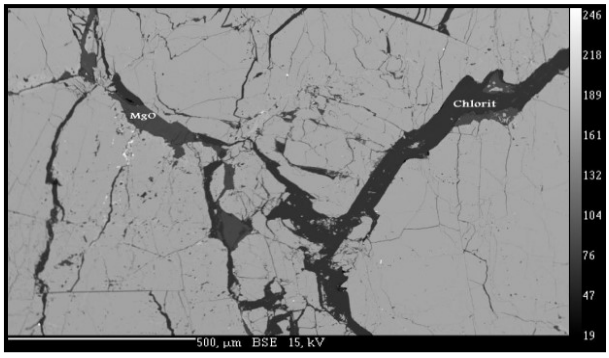

Fig 3. BSE image of sample no. 7 from Barantin-Rudan, combined with the mineral chlorite.

Minerals containing chromium garnets are called uvarovite. This mineral was identified as green coating on the surface of sample 2 and 9. With a theoretical structural formula of Ca_3 Cr_2 $[SiO_4]_3$, uvarovite contains 36 wt. % SiO_2, 30.4 wt. % Cr_2O_3, and 33.6 wt. % CaO. A comparison of these data with those from the chemical analysis (Table 5) shows only for Cr_2O_3 with 20.3 wt. %, a relative deviation of about 50%. The deviation has been considered at about 10%. The content of other elements Al and Fe, which can be as known as a replacement for Cr in the lattice of garnet, is about 6 wt. %. (Akizawa et al. 2016) reported uvarovite structures in ophiolites from Oman with a ratio for Cr / (Cr + Al + Fe) ranging from 0.5-0.6. For this study the ratio is 0.77 for garnet minerals. On the origin of these chromium-containing garnets, exsolution separation of iron oxide from the chromite would be conceivable. This process is preceded by the previous remobilization of Mg. By supplying CaO and SiO_2-containing solutions in the remaining structure (tetrahedral layer) probably formed uvarovite. This phenomenon is not detectable, but due to similar crystal systems between spinel and uvarovite (cubic) is conceivable.

4.2. The chemical composition of ore samples

The results of chemical analysis are presented in Table 3. Chrome ores are characterized by high Cr_2O_3 (26.9-49.8 wt. %) and MgO contents (15.1-26.1 wt. %). Fe_2O_3 and Al_2O_3 contents range between 11.0 - 16.3 wt. % and 6.6 - 19.1 wt. %. SiO_2 and LOI contents (difference to 100 wt. %: 100 - sum), which indicate the amount of coexisting silicates such as serpentine

and chlorite, which were between 4.3 – 24.7 wt. % and 2.3 – 5.2 wt. % respectively. One of the characteristic features of chromitites is the absent of Na and K and the low CaO content (0 – 2.9 wt. %). For the TiO_2 - low values have been recorded (0.12 to 0.24 wt. %). This is the case even more so for the P_2O_5 - content (0.02 to 0.04 wt. %). When comparing the levels of trace elements Ni, Co, and V, Ni has the highest content. Cu occurs only in one sample with 0.17 wt. % (sample 5). Assuming a Clarke-value of 30 wt. % (Wedepohl 1995) for the mine ability, in Cr ore can be seen in only one sample that does not satisfy this condition (sample 4).

Table 3. Chemical composition of the Cr ores by XRF (wt. %)

Sample Name	Z.N.G	NJ	RX	MJ	FB	SF	RB	FAR 3	FAR 1	FAR 2
Sample No.	1	2	3	4	5	6	7	8	9	10
SiO_2	18.10	4.28	19.95	24.67	20.09	18.42	8.99	6.82	8.13	13.49
Al_2O_3	10.72	19.12	8.80	6.84	6.56	7.16	9.44	8.52	12.40	7.12
MnO	0.13	0.14	0.17	0.10	0.16	0.12	0.09	0.14	0.14	0.12
MgO	18.08	15.08	17.84	26.12	23.56	23.20	20.76	16.00	15.16	19.88
CaO	-	0.96	2.88	0.20	0.88	0.04	-	0.16	0.08	0.20
TiO_2	0.24	0.20	0.24	0.12	0.16	0.12	0.12	0.12	0.16	0.12
P_2O_5	0.02	0.03	0.02	0.04	0.04	0.02	0.03	0.03	0.03	0.03
∑Fe as Fe_2O_3	15.68	14.68	15.28	11.04	14.88	12.72	12.48	15.20	16.32	13.48
Ni	0.17	0.15	0.11	0.20	0.42	0.18	0.18	0.11	0.12	0.12
Co	0.06	0.06	0.06	0.05	0.06	0.06	0.06	0.06	0.06	0.06
Cr_2O_3	31.57	42.92	29.68	26.88	30.08	34.24	45.04	49.83	43.55	41.43
Cu	-	-	-	-	0.17	-	-	-	-	-
V	0.05	0.06	0.05	0.03	0.04	0.04	0.03	0.06	0.07	0.05
Total	94.82	97.68	95.08	96.29	97.14	96.03	97.22	97.05	96.22	96.10

Table 4. Chemical components for spinel phases from the microprobe analysis (wt. %.).Mean values from different numbers (in the clip) of data points and standard deviation (STDEV).

Sample Name	Sample No.	MnO	MgO	NiO	Al_2O_3	Cr_2O_3	$FeO_{(tot.)}$	Structure formula
ZNG	1	0.17	14.84	0.15	12.38	54.48	16.82	$(Mg_{0.72}Ni_{<0.01}Mn_{<0.01}\ Fe^{2+}_{0.34})$
STDEV		±0.01(28)	±0.12(28)	±0.01(28)	±0.09(28)	±0.46(28)	±0.23(28)	$(Fe^{3+}_{0.12}Al_{0.48}Cr_{1.40})O_4$
NJ	2	0.14	15.09	0.15	20.80	49.37	13.47	$(Mg_{0.70}Ni_{<0.01}Mn_{<0.01}\ Fe^{2+}_{0.31})$
STDEV		±0.02(30)	±1.44(30)	±0.03(30)	±2.08(30)	±2.47(30)	±0.73(30)	$(Fe^{3+}_{0.04}Al_{0.76}Cr_{1.21})O_4$
RX	3	0.23	12.45	0.07	11.71	55.22	19.04	$(Mg_{0.62}Ni_{<0.01}Mn_{0.01}\ Fe^{2+}_{0.44})$
STDEV		±0.02(19)	±0.50(19)	±0.01(19)	±0.16(19)	±0.43(19)	±0.61(19)	$(Fe^{3+}_{0.09}Al_{0.46}Cr_{1.44})O_4$
MJ	4	0.19	13.72	0.08	13.46	56.49	16.21	$(Mg_{0.66}Ni_{<0.01}Mn_{<0.01}\ Fe^{2+}_{0.37})$
STDEV		±0.01(40)	±0.25(40)	±0.01(40)	±0.34(40)	±0.37(40)	±0.28(40)	$(Fe^{3+}_{0.06}Al_{0.51}Cr_{1.43})O_4$
FB	5	0.22	12.31	0.07	10.96	55.62	19.33	$(Mg_{0.61}Ni_{<0.01}Mn_{0.01}\ Fe^{2+}_{0.44})$
STDEV		±0.01(22)	±0.11(22)	±0.02(22)	±0.42(22)	±0.53(22)	±0.22(22)	$(Fe^{3+}_{0.06}Al_{0.43}Cr_{1.46})O_4$
SF	6	0.21	14.22	0.07	6.46	60.69	17.73	$(Mg_{0.71}Ni_{<0.01}Mn_{0.01}\ Fe^{2+}_{0.37})$
STDEV		±0.02(27)	±3.11 (27)	±0.01(27)	±3.87(27)	±3.09(27)	±2.69(27)	$(Fe^{3+}_{0.13}Al_{0.26}Cr_{1.58})O_4$
RB	7	0.14	16.34	0.16	10.32	58.17	13.27	$(Mg_{0.79}Ni_{<0.01}Mn_{<0.01}\ Fe^{2+}_{0.26})$
STDEV		±0.01(21)	±0.08(21)	±0.02(21)	±0.07(21)	±0.48(21)	±0.19(21)	$(Fe^{3+}_{0.10}Al_{0.40}Cr_{1.50})O_4$
Far 3	8	0.18	13.37	0.09	8.81	61.25	16.54	$(Mg_{0.65}Ni_{<0.01}Mn_{<0.01}\ Fe^{2+}_{0.38})$
STDEV		±0.03(18)	±2.38(18)	±0.02(18)	±2.11(18)	±1.55(18)	±2.73(18)	$(Fe^{3+}_{0.07}Al_{0.34}Cr_{1.59})O_4$
Far 1	9	0.17	12.85	0.09	10.95	58.99	16.45	$(Mg_{0.63}Ni_{<0.01}Mn_{<0.01}\ Fe^{2+}_{0.40})$
STDEV		±0.01(26)	±1.90(26)	±0.05(26)	±2.24(26)	±3.06(26)	±0.54(26)	$(Fe^{3+}_{0.05}Al_{0.42}Cr_{1.53})O_4$
Far 2	10	0.17	14.00	0.08	10.28	59.91	15.95	$(Mg_{0.68}Ni_{<0.01}Mn_{<0.01}\ Fe^{2+}_{0.35})$
STDEV		±0.02(16)	±0.47(16)	±0.03(16)	±1.72(16)	±2.30(16)	±0.20(16)	$(Fe^{3+}_{0.08}Al_{0.39}Cr_{1.53})O_4$

Plotted in Fig 4 is the Cr_2O_3 against SiO_2 content of the total chemical analysis. The relatively good correlation coefficient of 0.8768 shows that it is possible with sufficient accuracy to determine the Cr_2O_3 content of the ore from the SiO_2-value of the overall analysis and estimate the mine ability of chrome ore reliable.

Figure 5 shows the correlation between MgO and Fe_2O_3 content of the overall chemistry, determined by the XRF method. When creating structural formulas for spinel it has been noted that Mg and Fe are to be (mainly in the divalent form) considered as components of the octahedral cations. The paragenesis of the silicate minerals, mainly serpentine and chlorite with preserved olivine and diopside shares are in addition to the spinel essential carrier of Mg and Fe^{2+} (Deer et al. 1992). Even in this case, namely the presence of silicate phases in the formation of the ores from the melt has an opposite behavior than expected of Fe and Mg. The relationship with the linear correlation coefficient of 0.607 (Fig 5) reveals in the broadest sense the fact that with increasing incorporation of Mg in the octahedral decreases the proportion of octahedral Fe. A conceivable explanation would be since the behavior, according to the Goldschmidt's rule to which there is a presence of two ions of similar size and charge, the smaller ion can easily penetrate into a given crystal lattice (Duke 1983).

The above hypothesis can be confirmed if one uses the appropriate data from the microprobe analysis, and this resulted in the diagram (Fig 6) to be compared with the diagram in Fig 5. As can be seen from Fig 6, we obtained almost the same linear profile with a slightly better correlation coefficient (R^2 = 0.6896), which is why the points are closer to the regression line. One such relationship is with other cation pairs such Al/Fe^{3+}, either none or hardly any, will be omitted at this point in the presentation of corresponding diagrams. It should be noted, that for the Al/Fe^{3+} ratio of the spinel phases, the proportion of Fe^{3+} in comparison with Al comparatively low fails.

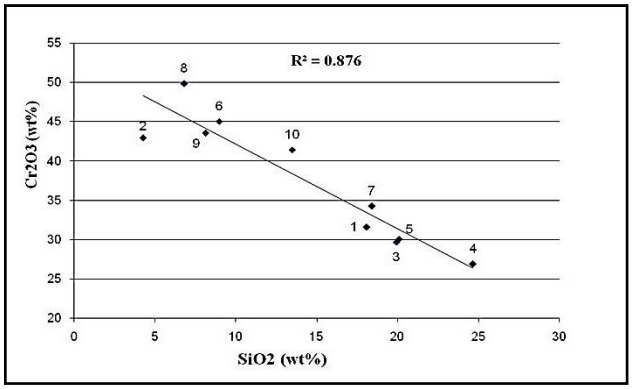

Fig 4. Cr_2O_3 / SiO_2, Correlation diagram from XRF (numbers on the black circles denote sample number)

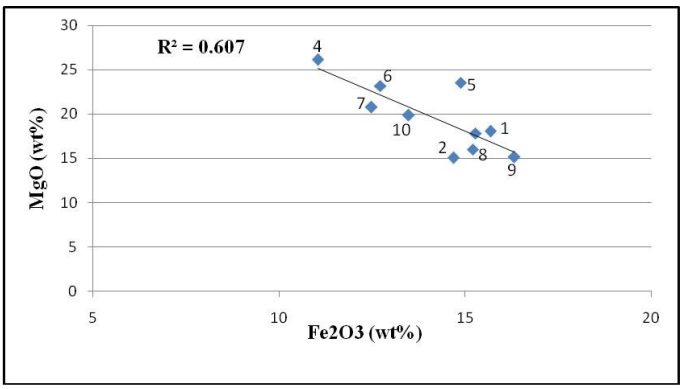

Fig 5. Correlation between MgO / Fe_2O_3 from the XRF (numbers on the black circles denote sample number)

Table 5. The chemical composition of primary and secondary silicates in wt. % (digit in parentheses shows the number of point measurements-data from Tarrah and Abedpour (2014)

Chem	Olivine [a)]	Pyroxene [b)]	Serpentine [c]	Chlorite [d)]	Uvarovite[e)]
Composition	**(37)**	**(18)**	**(47)**	**(47)**	**(22)**
SiO2	41.10	54.05	40.10	32.90	36.00
TiO2	0.00	0.05	0.00	0.05	2.10
Al2O3	0.05	0.80	0.30	15.10	3.80
Cr2O3	0.01	0.70	0.20	3.10	20.30
∑ Fe as FeO	5.90	1.00	2.50	1.30	2.05
MnO	0.07	0.03	0.03	0.01	0.01
NiO	0.50	0.10	0.30	0.20	0.00
CaO	0.00	24.50	0.00	0.10	34.50
MgO	52.50 Fo (Mg): 89.90	18.40 Wo (Ca): 57.1	41.90	35.10	0.20
Total	100.1	99.6	85.8	88.5	99.3

a): Average for samples 1/3/5/10, b): Average for samples 4/5, c): Average for samples 1/3/4/6/8/10, d): Average for samples 2/5/6/7/8/9, e): Average for samples 2/9, Fo: Forsterite, Wo: Wollastonite.

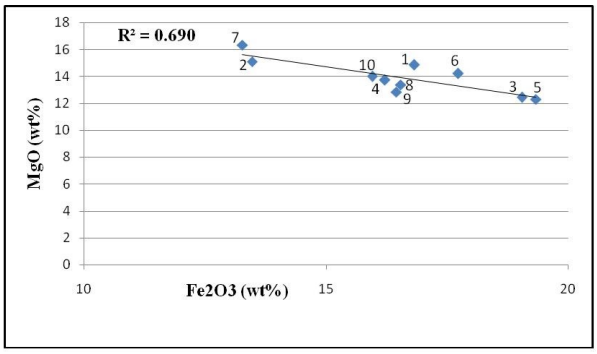

Fig 6. Correlation between Mg/Fe from the microprobe analysis of spinel (numbers on the black circles denote sample number)

4.3. The chemistry of the spinel

The results for the chemical composition of the spinel phase of the microprobe analysis and the resulting structural formulas are shown in the Table 4. The mean values for the oxide contents, the standard deviation and the number of point measurements are also listed.

According to the data in the literature, the ratios of Cr/ (Cr+Al) and Mg/ (Mg+Fe^{2+}) were calculated and multiplied because of the simplicity with 100 for the classification of podiform chromites. In the presented chromites, the following mean values are:

Cr # [100 × (Cr / Cr + Al) = 75-92] and Mg # [100×(Mg / Mg + Fe^{2+}) = 38-57]

For the chromium deposits Faryab (southeast Iran) from which the samples (number 5, 8, 9, and 10) studied here originated was identified based on the following values from and (Rajabzadeh and Dehkordi 2013):

Cr # [100 × (Cr / Cr + Al) = 77-85] and Mg # [100×(Mg / (Mg + Fe^{2+}) = 56-73]

In the broadest sense, the chemical composition of the spinel reflects the type of naturally occurring chromium ores (Duke 1983; Zhou and Bai 1992; Zhou et al. 1996). In general, the chromite deposits depending on their origin are divided into two groups: (a) Podiform chromite deposits with irregular, mainly lenticular chromite-rich bodies that occur in alpine or ophiolite complexes and (b) Stratiform chromite deposits with laterally persistent chromite-rich layers alternating with silicate layers. Type a indicates a low content of Fe^{3+} and shows a characteristic Cr-Al substitution, while type b generally has more Fe^{3+}. In Figure 7, the Mg-number [Mg / (Mg + Fe^{2+})] was plotted against the Cr-number [Cr / (Cr + Al)]. The measurement points fall either in the common area (samples 1/3/4/5/9/10) or in the field of podiform chromites (samples 2/6/7/8). Comparisons of Al_2O_3 and TiO_2 contents for spinels of all of the samples except the sample 2 spinel plot in the arc basalts field are shown in (Fig 8) (Kamenetsky et al. 2001).

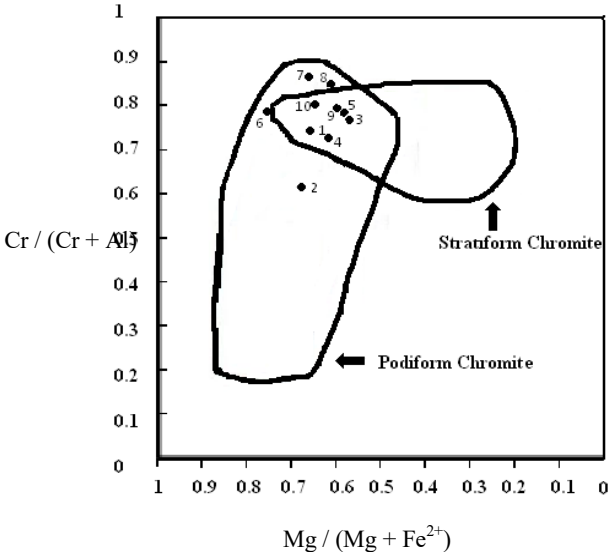

Fig 7. Chromites in the Mg / (Mg + Fe^{2+}) to Cr / (Cr + Al) diagram (numbers on the black circles denote sample number) - podiform and stratiform deposit fields [28].

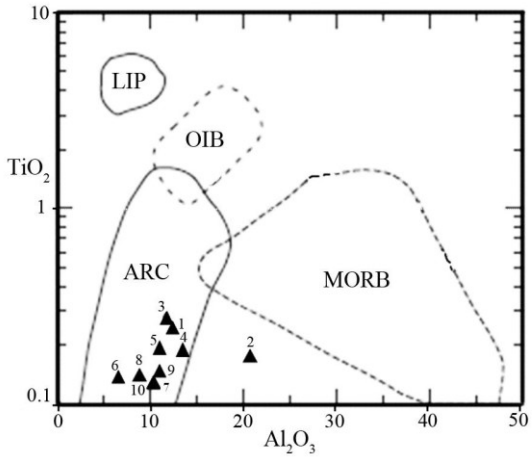

Fig 8. Al_2O_3 (wt. %) vs. TiO_2 (wt. %), fields are shown for spinels from large igneous provinces (LIP), ocean island basalt (OIB), arc basalts (Arc) and mid-ocean ridge basalts (MORB) [29]

From the structural formulas in Table 4, it has been observed that the spinel phases are not made of pure end members. ; rather, they are mixed crystals of the phases chromite ($Fe^{2+}Cr_2O_4$), magnesiochromite ($MgCr_2O_4$), spinel ($MgAl_2O_4$), and hercynite ($Fe^{2+}Al_2O4$). In this complex mineral chemistry is also a solid solution relationship with picotite [$(Mg,Fe^{2+})(Cr,Al,Fe^{3+})O_4$], which still incorporates Fe^{3+}in the tetrahedral position. Assuming that the Cr-mineral precipitated an early stage of the crystallization phase(Mason et al. 1985), the variation in chemical composition may probably be due to different compositions of the melt formation. However,

statements about origin are vague and limited in the methods used in this work. The main compositional variations are due to the substitution of Mg by Fe in the octahedral position (see Fig 6, section 4.2) or substitution of Cr by Al in the tetrahedral layer (Fig 9).

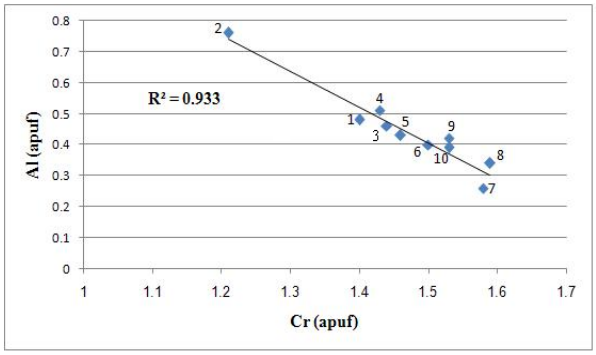

Fig 9. Al content vers. Cr content for spinel phases (apfu: Atom per formula unit O_4; numbers on the black circles denote sample number)

5. Conclusion

The determination of the structural formula of the spinel phase has an important role in the characterization of the Cr ores, and the use of these Cr-occurrences in the industry. The chemical composition in terms of structural formula provides the assessment and decision-making data for further exploration and exploitation. The relationships found here, however, are restricted and cannot be generalized without further notice. Such relationships need to be checked for spinels from different backgrounds, especially for the Fe-rich stratiform chromites. For this purpose, the distinction of Fe in two and trivalent form should not be done mathematically but analytically, such as by photometry. Therefore new aspects should be explored in further studies.

Acknowledgements

The authors are grateful to the Islamic Azad University of Bandar Abbas (Iran) and the technical University of Clausthal (Germany) for the approval of this research program and the financial support. Thanks are also due the S. Ghoreishi for data processing and the unknown reviewers.

References

Akizawa N, Tamura A, Fukushi K, Yamamoto J, Mizukami T, Python M, Arai S (2016) High-temperature hydrothermal activities around suboceanic Moho: an example from diopsidite and anorthosite in Wadi Fizh, Oman ophiolite, *Lithos*.

Bagherian S, Tourchi M (2004) A study of Chromite Deposits of the Abdasht Peridotites, *Journal of Earth Science* 11:108-115. (in Persion)

Deer WA, Howie RA, Zussman J (1992) An introduction to the rock-forming minerals vol 696. Longman London.

Duke J (1983) Ore deposit models 7: Magmatic segregation deposits of chromite, *Geoscience Canada* 10:15-24.

Emamalipour A (2008) Mineralogy of accessory and rare minerals associated with chromite deposits in the khoy area, *Iranian Journal of Crystallography and Mineralogy* 16:559-570.

Ghazi A, Hassanipak A, Mahoney J, Duncan R (2004) Geochemical characteristics, 40 Ar–39 Ar ages and original tectonic setting of the Band-e-Zeyarat/Dar Anar ophiolite, Makran accretionary prism, SE Iran, *Tectonophysics* 393:175-196.

Glennie K, Clarke MH, Boeuf M, Pilaar W, Reinhardt B (1990) Inter-relationship of Makran-Oman Mountains belts of convergence, *Geological Society, London, Special Publications* 49:773-786.

Glennie KW (2000) Cretaceous tectonic evolution of Arabia's eastern plate margin: a tale of two oceans.

Kamenetsky VS, Crawford AJ, Meffre S (2001) Factors controlling chemistry of magmatic spinel: an empirical study of associated olivine, Cr-spinel and melt inclusions from primitive rocks, *Journal of Petrology* 42:655-671.

Lameyre J (1986) Roches et minéraux: matériaux de la terre et témoins de son histoire. Doin Editeurs, París, 350 p. (in French)

Mason B, Moore CB, Hintermaier-Erhard G (1985) Grundzüge der Geochemie: 66 Tabellen. Enke.

McCall G (1997) The geotectonic history of the Makran and adjacent areas of southern Iran, *Journal of Asian Earth Sciences* 15:517-531.

McCall G (2002) A summary of the geology of the Iranian Makran, *Geological Society, London, Special Publications* 195:147-204.

McCall G, Kidd R (1982) The Makran, Southeastern Iran: the anatomy of a convergent plate margin active from Cretaceous to Present, *Geological Society, London, Special Publications* 10:387-397.

McCall GJH (1985) Explanatory Text of the Minab Quadrangle Map, 1: 250,000. Geological Survey of Iran.

Moghtaderi A, Khakzad A, Liaghat S (2003) Occurrence and geochemistry of Jamali-Mines-Neyris-Iran., *Geoscience* 11:47-48. (in Persion)

Mussallam K, Jung D, Burgath K (1981) Textural features and chemical characteristics of chromites in ultramafic rocks, Chalkidiki Complex (Northeastern Greece), *Tschermaks mineralogische und petrographische Mitteilungen* 29:75-101.

Okrusch M, Matthes S (2013) Mineralogie: eine Einführung in die spezielle Mineralogie, Petrologie und Lagerstättenkunde. Springer-Verlag.

Rajabzadeh MA, Dehkordi TN (2013) Investigation on mantle peridotites from Neyriz ophiolite, south of

Iran: geodynamic signals, *Arabian Journal of Geosciences* 6:4445-4461.

Rajabzadeh MA, Moosavinasab Z (2012) Mineralogy and distribution of Platinum-Group Minerals (PGM) and other solid inclusions in the Neyriz ophiolitic chromitites, Southern Iran, *The Canadian Mineralogist* 50:643-665.

Rajabzadeh MA, Moosavinasab Z (2013) Mineralogy and distribution of Platinum-Group Minerals (PGM) and other solid inclusions in the Faryab ophiolitic chromitites, Southern Iran, *Mineralogy and Petrology* 107:943-962.

Shafaii Moghadam H, Stern RJ (2015) Ophiolites of Iran: Keys to understanding the tectonic evolution of SW Asia:(II) Mesozoic ophiolites, *Journal of Asian Earth Sciences* 100:31-59.

Shahabpour J (2010) Tectonic implications of the geochemical data from the Makran igneous rocks in Iran, *Island Arc* 19:676-689.

Siddiqui RH, Jan MQ, Khan MA (2012) Petrogenesis of late Cretaceous lava flows from a Ceno-Tethyan island arc: The Raskoh arc, Balochistan, Pakistan, *Journal of Asian Earth Sciences* 59:24-38.

Tarrah J, Abedpour Z (2014) The study of the chemical composition from silicate phases in chrome ores, SE of Iran. 18th Symposium of the Geological Society of Iran, pp 916-923. (in Persion).

Wedepohl KH (1995) The composition of the continental crust, *Geochimica et Cosmochimica Acta* 59:1217-1232.

Zhou M-F, Bai W-J (1992) Chromite deposits in China and their origin, *Mineralium Deposita* 27:192-199.

Zhou M-F, Robinson PT, Malpas J, Li Z (1996) Podiform chromitites in the Luobusa ophiolite (Southern Tibet): implications for melt-rock interaction and chromite segregation in the upper mantle, *Journal of Petrology* 37:3-21.